Journal of Power Sources 196 (2011) 8402–8405

Contents lists available at ScienceDirect

Journal of Power Sources

journal homepage: www.elsevier.com/locate/jpowsour

Short communication

Mechanical strengthening of Sm-doped CeO_2 ceramics by 1 mol% cobalt oxide for solid oxide fuel cell application

Yingchao Dong[a,*], Stuart Hampshire[a], Jian-er Zhou[b], Xinfa Dong[d], Bin Lin[c], Guangyao Meng[c]

[a] Materials and Surface Science Institute (MSSI), University of Limerick (UL), Ireland
[b] Key Lab of Jiangxi Universities for Inorganic Membranes, Jingdezhen Ceramic University, China
[c] USTC Lab for Solid State Chemistry and Inorganic Membranes, University of Science and Technology of China (USTC), China
[d] School of Chemistry and Chemical Engineering, South China University of Technology (SCUT), China

ARTICLE INFO

Article history:
Received 15 February 2011
Received in revised form 23 April 2011
Accepted 3 June 2011
Available online 13 June 2011

Keywords:
SOFC electrolyte
Sm-doped CeO_2
CoO co-doping
Mechanical strengthening

ABSTRACT

Combustion processed nano-sized $Ce_{0.79}Sm_{0.20}Co_{0.01}O_{2-\delta}$ (CSCoO) and $Ce_{0.80}Sm_{0.20}O_{2-\delta}$ (CSO) were sintered at various temperatures, and mechanical properties and microstructures were characterized. The results demonstrate that besides a lowering of sintering temperature to achieve sufficient densification, the doping of very minor amounts of CoO (1 mol%) to CSO significantly enhanced mechanical properties. The CSCoO sintered at 1100 °C exhibits a biaxial flexural strength of 354 ± 42 MPa which compared with 194 ± 57 MPa for CSO with a similar relative density sintered at 1400 °C. This slight modification in chemical composition also resulted in a slight improvement in micro-hardness.

1. Introduction

In the past decades, CeO_2-based ceramics doped with rare earth elements have been widely studied as promoter for heterogeneous catalytic reactions [1] and as electrolytes for solid oxide fuel cells (SOFCs) [2]. Among them, Sm-doped CeO_2 is an upcoming alternative to yttria-stabilized zirconia (YSZ) as solid electrolyte for intermediate temperature SOFCs, owing to high conductivity, good chemical compatibility and low operating temperature [3]. To prepare dense CeO_2 based electrolytes, various strategies have been extensively studied including: (1) adoption of high activity powders [4,5]; (2) specific process treatments [6,7]; (3) addition of sintering aids [8,9]. However, while CSO ceramics have high conductivities at intermediate and low temperatures compared with YSZ, they typically exhibit poor mechanical properties due to thermo-mechanical stresses introduced during cell fabrication and operation. This has severely limited their application and inhibited the commercialization of ceria-based SOFCs. To date, only a few studies have focused on mechanical strengthening of ceria-based electrolytes. Zhang et al. [10] and Kang and Choi [11] reported that Al_2O_3 could be used as a strengthening additive to improve the mechanical properties of $Ce_{0.8}Gd_{0.2}O_{2-\delta}$ (CGO) but this needs over 10% $AlO_{1.5}$ without decreasing densification temperature.

High electrical conductivity can be achieved for 20 mol% Sm doped ceria, i.e. $Ce_{0.80}Sm_{0.20}O_{2-\delta}$ (CSO) [12]. The minor doping of 1 mol% Co into 20CGO ($Ce_{0.8}Gd_{0.2}O_{2-\delta}$) could decrease densification temperature, as well as improve total electrical conductivity [13]. In this communication, by adding very small amounts of dopant CoO (1 mol%) to CSO, a slight compositional modification into $Ce_{0.79}Sm_{0.20}Co_{0.01}O_{2-\delta}$ (CSCoO) was adopted in order to improve mechanical properties. Sintering densities, flexural strengths, microhardness and electrical conductivity of CSO and CSCoO were measured and conclusions regarding the underlying fracture mechanisms are proposed based on SEM analysis.

2. Experimental

Both CSO and CSCoO powders were synthesized by the PVA combustion method using the following procedures [14]. Appropriate proportions of $Ce(NO_3)_3{\cdot}6H_2O$ (≥99.0%), $Co(NO_3)_2{\cdot}6H_2O$ (≥99+%) and Sm_2O_3 (99.9%) were dissolved in distilled water and dilute nitric acid, respectively. 5.00 wt.% aqueous PVA (typical Mw 89,000–98,000, 99+% hydrolyzed) solution was added to the mixed metal nitrate solution with PVA monomer to cations ratio of 2:1. Excess water was vaporized during the homogenization of this solution at 90 °C, then transferred into a 1000 ml ceramic basin above an electrical furnace. The combustion reaction took place dramatically in an instant. The as-synthesized powders were calcined at 600 °C for 2 h, followed by attrition-milling in distilled water for 2 h at a speed of 600 rpm min^{-1}, then dried at 120 °C for

* Corresponding author. Tel.: +353 866694013; fax: +353 61338172.
E-mail addresses: yingchao.dong@ul.ie, dongyc9@mail.ustc.edu.cn (Y. Dong).

0378-7753/$ – see front matter © 2011 Elsevier B.V. All rights reserved.
doi:10.1016/j.jpowsour.2011.06.012

24 h. CSCoO and CSO pellets (⌀ 20 mm) were uniaxially pressed and then sintered in air for 5 h at 900–1100 °C and at 1200–1400 °C, respectively.

The relative density was calculated using the relation % density = $(d_b/d_{th}) \times 100$, where d_b is the bulk density (using the Archimedes' method) and d_{th} is the theoretical density given by the following equations:

$$d_{th,CSO} = \left(\frac{4}{N_A a^3}\right)\left((1-x)M_{Ce} + xM_{Sm} + \left(\frac{2-x}{2}\right)M_O\right) \quad (1)$$

$$d_{th,CSCoO} = \left(\frac{4}{N_A a^3}\right)\left((1-x-y)M_{Ce} + xMSm + yM_{Co} + \left(\frac{2-x}{2}\right)M_O\right) \quad (2)$$

where x is Sm content ($x = 0.2$), y is Co content ($y = 0.01$), a is the lattice parameter calculated from XRD data, N_A is Avogadro's number (6.022×10^{23}), and M_X is the atomic weight of atom X (Ce, Sm, Co and O).

Biaxial flexural strength tests were performed according to ISO 6872 [15] on disc specimens (diameters: 15–17 mm; thicknesses: 0.70–0.85 mm). A load frame (Lloyd LR50K, UK) with a crosshead speed of 0.1 mm min^{-1} and a preload of 2N was utilised along with a test jig with a support radius of 4.1 mm. Samples were polished using 400-mesh, then 800-mesh metallographic sandpapers, followed by CeO_2 polishing paste (1 μm). Vickers hardness tests were performed using a diamond indentation technique with a load of 200–300 N for 10 s (10 indents per composition, across 3 different samples) [16].

SEM (SU70 FE-SEM, Hitachi) observations were performed on the fracture surfaces (after strength test) and surfaces (after hardness test) of CSO sintered at 1400 °C for 5 h (CSO-1400) and CSCoO sintered at 1100 °C for 5 h (CSCoO-1100). The average grain size, G, was determined using the relation:

$$G = \frac{1.5L}{M \cdot N} \quad (3)$$

where 1.5 is a geometry-dependent proportionality constant, L is the total test line length, M is the magnification and N is the total number of intercepts.

3. Results and discussion

Fig. 1 presents the relative densities of the CSO and CSCoO compacts sintered at different temperatures. For CSO, a rapid increase in relative density is observed from 76.0 ± 2.3% at 1200 °C to 93.1 ± 1.4% at 1300 °C, indicating a significant densification. At 1400 °C, a maximum relative density of 96.6 ± 1.6% is reached. Compared with CSO, the densification of CSCoO was achieved at much lower temperatures. The CSCoO sintered at 1100 °C possesses a relative density of 94.6 ± 1.1%. This significant reduction of 300 °C in densification temperature can be ascribed to the sintering-aid function of CoO as observed previously [17]. Above 1100 °C, the relative density of CSCoO remains unchanged basically with temperature.

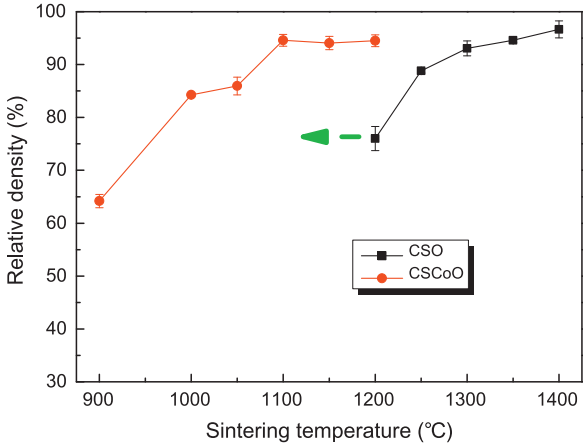

Fig. 1. Relative densities of the CSCoO and CSO sintered bodies as a function of temperature.

Fig. 2 shows the results of biaxial flexural strength tests for CSO and CSCoO. The enhancements of strength with sintering temperature can be clearly seen (Fig. 2a), with a maximum strength of 194 ± 57 MPa for CSO sintered at 1400 °C compared with 354 ± 42 MPa for CSCoO sintered at a much lower temperature of only 1100 °C; the strength of CSCoO is 82.5% higher than that of CSO. The flexural strength of CSO in this work is close to that of the oxalate coprecipitation processed CSO [18], which is much higher than that reported by Sameshima et al. (53–81 MPa) [19]. The doping of 5 mol% Y into CSO ($Ce_{0.80}Sm_{0.15}Y_{0.05}O_{2-\delta}$) degraded bending strength [20]. As reported by Cutler et al. [21], reaction-sintered Ti–Sm co-doped CeO_2 ($Ce_{0.84}Sm_{0.15}Ti_{0.01}O_{1.925}$) exhibits an increased biaxial flexural strength of 250 MPa. By comparison, the strength of Co–Sm co-doped CeO_2 in this work is as high as 354 ± 42 MPa when sintered at a much lower temperature of 1100 °C for 5 h.

In Fig. 2b, both CSO and CSCoO exhibit trends of increasing strength with increasing relative density. However, even at the same relative densities, CSCoO exhibits much higher strength than

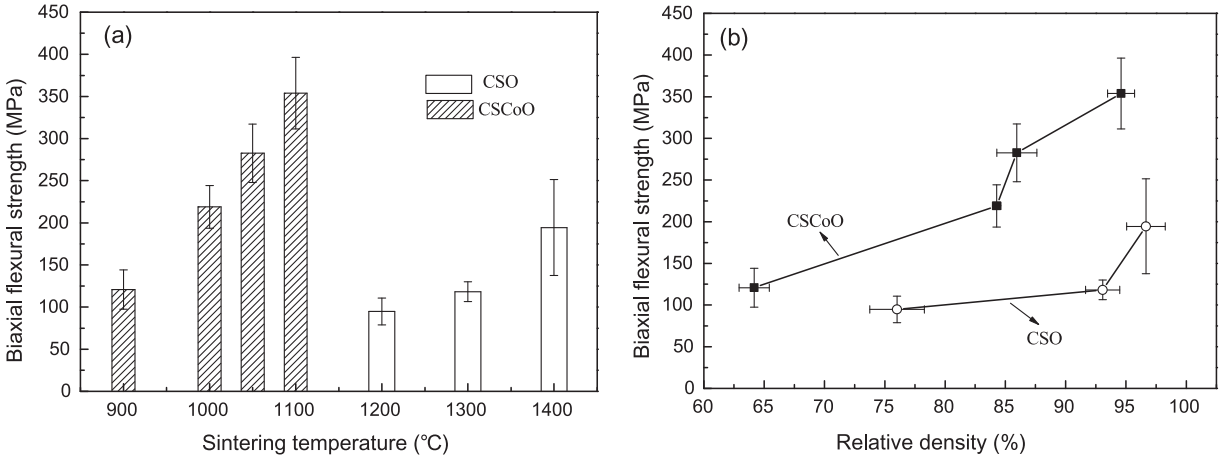

Fig. 2. Biaxial flexural strength results for CSO and CSCoO: (a) strength versus sintering temperature and (b) strength versus relative density.

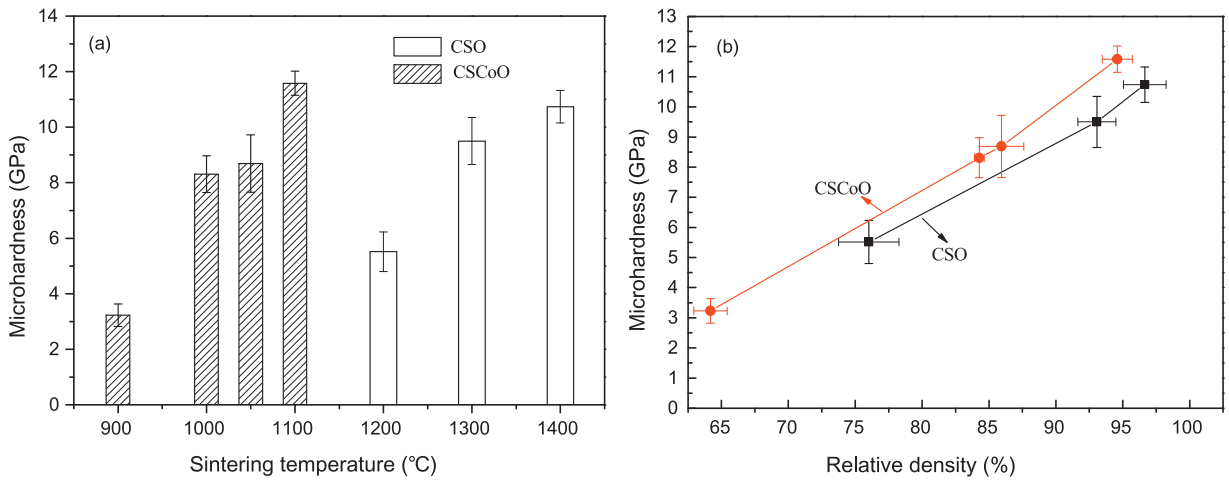

Fig. 3. Microhardness of CSO and CSCoO sintered bodies: (a) hardness versus sintering temperature and (b) hardness versus relative density.

CSO. Such improvements imply that other factors, except for porosity, are responsible for the increases in strength of CSCoO.

Fig. 3 presents the microhardness results of CSO and CSCoO. From Fig. 3a, the CSO exhibits an increase in microhardness with sintering temperature from 5.51 ± 0.72 GPa at 1200 °C to a maximum of 10.74 ± 0.59 GPa at 1400 °C. The hardness of CSCoO increases from 3.23 ± 0.41 at 900 °C to 8.69 ± 1.03 GPa at 1050 °C and then reaches the highest value of 11.58 ± 0.44 GPa at 1100 °C. At the same relative densities (Fig. 3b), CSCoO exhibits slightly higher hardness than CSO. This shows once again that CSCoO possesses better mechanical properties than CSO.

Fig. 4 shows the fractographic and surface images of CSO-1400 and CSCoO-1100 after strength and hardness tests. In CSO (Fig. 4a and c) the white arrows and circles, respectively, indicate several typical regions of intergranular and transgranular fracture modes. Intergranular crack propogation by brittle fracture is more prevalent in CSO and leads to the separation of grain boundaries with smooth fracture surfaces, while due to the separations of single grains during fracture, transgranular mode of crack growth generates rough fracture surfaces (Fig. 4b and its insert) [22] which is the predominant fracture mode in CSCoO, also well justified in Fig. 4d. The average grain sizes of CSO-1400 and CSCoO-1100 are 0.96 ± 0.04 μm and 0.61 ± 0.05 μm. This enhancement of mechanical property may be related to the change from intergranular fracture (CSO) to transgranular fracture (CSCoO) due to the doping of 1mol% CoO. As a follow-up to this work, a microstructural investigation is under way in order to understand more fully the changes in fracture mode.

Fig. 5 shows the Arrhenius plots of $\ln(\sigma T)$ versus $1000/T$ for CSO-1400 and CSCoO-1100. The total conductivities of CSO-1400 and CSCoO-1100 were 0.0065 S cm^{-1} and 0.0090 cm^{-1} at 600 °C, indicating that the CoO doping could also improve electrical performance of PVA processed CSO, but this improvement is not as high as that reported by Dutta et al. [13],

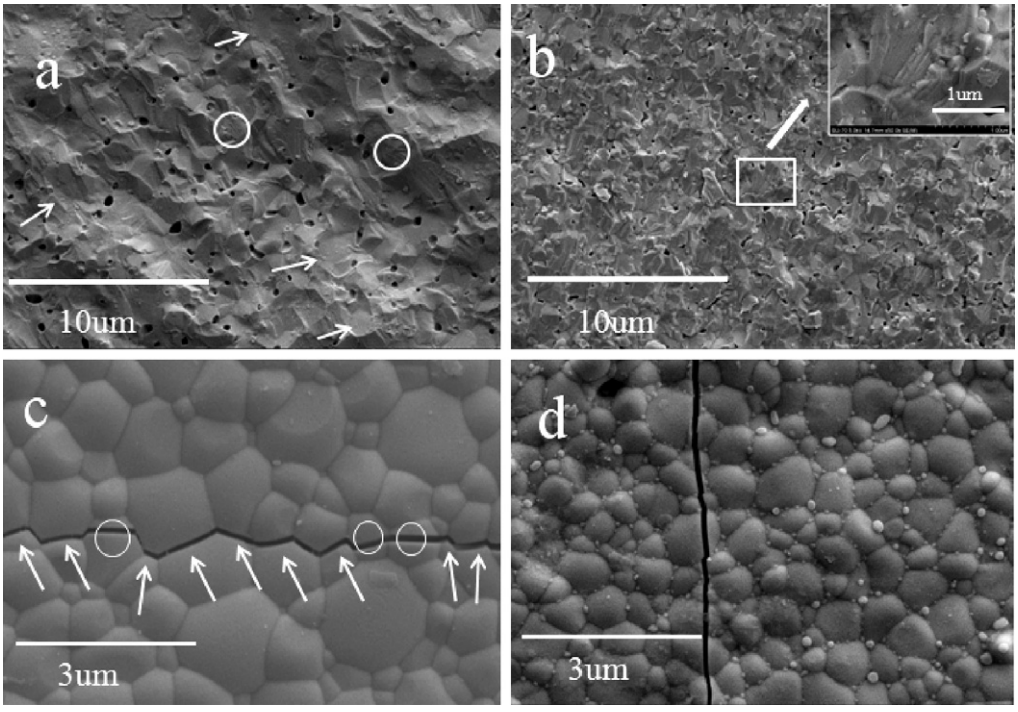

Fig. 4. SEM micrographs of the fracture surfaces (after strength test) and surfaces (after hardness test) of CSO-1400 and CSCoO-1100: (a) fracture surface of CSO-1400; (b) fracture surface of CSCoO-1100; (c) surface of CSO-1400 and (d) surface of CSCoO-1100.

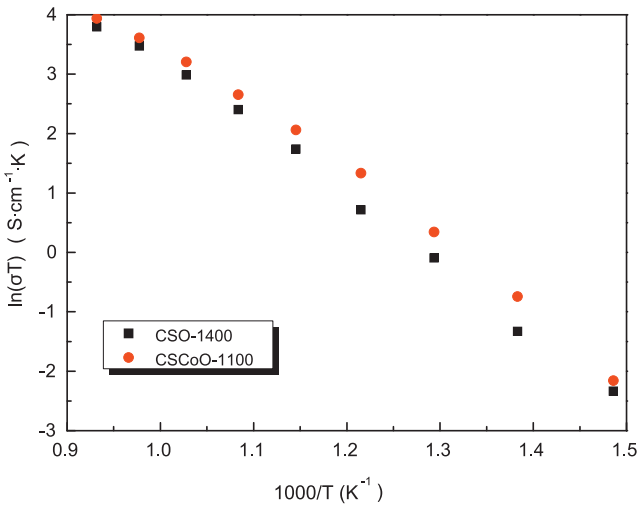

Fig. 5. Arrhenius plots of ln(σT) versus 1000/T for the CSO sintered at 1400 °C (CSO-1400) and the CSCoO sintered at 1100 °C (CSCoO-1100).

where nano-sized CGCoO was synthesized by the citrate–nitrate method.

4. Conclusions

A slight compositional modification of CSO into CSCoO by doping with 1 mol.% CoO offered two advantages: (1) decreased densification temperature; a significant reduction in sintering temperature was obtained from 1400 °C for CSO to 1100 °C for CSCoO and (2) significantly enhanced mechanical properties; the flexural strength was significantly increased even at much lower sintering temperatures by doping with CoO. Moreover, this slight modification in composition also resulted in a slight improvement in microhardness. The improvement of mechanical properties can be ascribed to two different fracture mechanisms: a complete transgranular mode for CSCoO, and the mixed type of intergranular (dominant) and transgranular mode for CSO.

Acknowledgments

The authors wish to thank the Irish Research Council for Science, Engineering and Technology through an EMPOWER Post-doctoral Fellowship (YD) and China Post-Doctoral Grant Scheme (contract no. 20100470846) for financial support.

References

[1] M. Kobune, S. Sato, R. Takahashi, J. Mol. Catal. A: Chem. 279 (2008) 10.
[2] N.Q. Minh, J. Am. Ceram. Soc. 76 (1993) 563.
[3] B.C.H. Steele, A. Heinze, Nature 414 (2001) 345.
[4] Z. Gao, J.B. Huang, Z.Q. Mao, C. Wang, Z.X. Liu, Int. J. Hydrogen Energy 35 (2010) 731.
[5] J.J. Ma, C.R. Jiang, X.L. Zhou, G.Y. Meng, X.Q. Liu, J. Power Sources 162 (2006) 1082.
[6] W.S. Jung, H.S. Park, Y.J. Kang, D.H. Yoon, Ceram. Int. 36 (2010) 371.
[7] J.P. Liang, Q.S. Zhu, Z.H. Xie, W.L. Huang, C.Q. Hu, J. Power Sources 194 (2009) 640.
[8] X.G. Zhang, C. Dec'es-Petit, S. Yick, M. Robertson, O. Kesler, R. Maric, D. Ghosh, J. Power Sources 162 (2006) 480.
[9] V. Esposito, M. Zunic, E. Traversa, Solid State Ionics 180 (2009) 1069.
[10] T.S. Zhang, Z.Q. Zeng, H.T. Huang, P. Hing, J. Kilner, Mater. Lett. 57 (2002) 124.
[11] Y.J. Kang, G.M. Choi, Solid State Ionics 180 (2009) 886.
[12] H. Inaba, H. Tagawa, Solid State Ionics 83 (1996) 1.
[13] A. Dutta, A. Kumar, R.N. Basu, Electrochem. Commun. 11 (2009) 699.
[14] Y.C. Dong, S. Hampshire, B. Lin, Y.H. Ling, X.Z. Zhang, J. Power Sources 195 (2010) 6510.
[15] CEN. Dental ceramic (ISO 6872-1995). In: Standardization ECf, editor, 1998.
[16] D.J. Curran, T.J. Fleming, M.R. Towler, S. Hampshire, J. Mater. Sci.: Mater. Med. 21 (2010) 1109.
[17] C. Kleinlogel, L.J. Gauchler, Adv. Mater. 13 (2001) 1081.
[18] T. Ishida, F. Iguchi, K. Sato, T. Hashida, H. Yugami, Solid State Ionics 176 (2005) 2417.
[19] S. Sameshima, T. Ichikawa, M. Kawaminami, Y. Hirata, Mater. Chem. Phys. 61 (1999) 31.
[20] M. Dudek, W. Bogusz, Ł. Zych, B. Trybalska, Solid State Ionics 179 (2008) 164.
[21] R.A. Cutler, D.L. Meixner, B.T. Henderson, K.N. Hutchings, D.M. Taylor, M.A. Wilson, Solid State Ionics 176 (2005) 2589.
[22] C.D. Beachem, Fracture 1, Academic Press, Liebowitz, 1968, pp. 243–249.